Supramolecular assembly of $[Cu(2,2'\text{-bpy})_2(ppac)](H_2O)_7$ (1) and $[Cu_2(2,2'\text{-bpy})_4(ppac)]( )_2(H_2O)_{16}$ (2) with unprecedented water morphologies

Fei-Long Hu [a] , Xin Yang [b] & Yong-Jun Li [c]

[a] College of Chemistry and Materials, Yulin Normal University , Yulin 537000 , PR China

[b] Department of Chemistry and Chemical Engineering , Huaihua College , Huaihua 418000 , PR China

[c] Zhongshan Quality Supervision & Inspection Institute of Agricultural Products , Zhongshan 528403 , PR China
Accepted author version posted online: 12 Oct 2012.Published online: 25 Oct 2012.

PLEASE SCROLL DOWN FOR ARTICLE

Supramolecular assembly of [Cu(2,2′-bpy)$_2$(ppac)](H$_2$O)$_7$ (1) and [Cu$_2$(2,2′-bpy)$_4$(ppac)](HCO_2^-)$_2$(H$_2$O)$_{16}$ (2) with unprecedented water morphologies

FEI-LONG HU*†, XIN YANG‡ and YONG-JUN LI§

†College of Chemistry and Materials, Yulin Normal University, Yulin 537000, PR China
‡Department of Chemistry and Chemical Engineering, Huaihua College,
Huaihua 418000, PR China
§Zhongshan Quality Supervision & Inspection Institute of Agricultural Products,
Zhongshan 528403, PR China

In this article, two copper(II) complexes, [Cu(2,2′-bpy)$_2$(ppac)](H$_2$O)$_7$ (**1**) and [Cu$_2$(2,2′-bpy)$_4$ (ppac)](HCO_2^-)$_2$(H$_2$O)$_{16}$ (**2**), have been synthesized (H$_2$ppac = p-phenylenediacetic acid, 2,2′-bpy = 2,2′-bipyridine). We report structural evidence of discrete water clusters in the solid state. An unusual 1-D water tape notated T4(2)6(2) is present in complex **1**. Complex **2** displays a hydrogen-bonded pillar-layered structure that is constituted by lattice waters. An unprecedented water cluster notated as T4(1)6(1)6(2) is present in complex **2**. The units act as supramolecular glue in the aggregation of copper(II) complexes to give a 3-D cage-like network through hydrogen bonds. Preliminary investigation on electrochemical properties of the complexes is presented.

Keywords: Water cluster; Negative charge; Complexes; Pillar-layer

1. Introduction

Water has been thoroughly investigated due to its importance in many biological, chemical, and physical processes [1]. Attention has been focused on theoretical [2, 3] and experimental [4–7] studies of small water clusters to understand the structures and characteristics of liquid water and ice [8–10]. A variety of tetramer, pentamer [11], hexamer, octamer [12–15], and decamer water clusters have been isolated in different crystalline hosts. Water clusters play important role in stabilization of supramolecular systems both in solution and in the solid state, and there is clearly a need for a better understanding of how such water aggregations are influenced by the overall structure of their surroundings [16–18].

For water morphologies, tetramers and hexamers are common with a large number of water structures containing water tetramers such as T4(0)A2 [19], T4(1),

---

and T4(2)6(2) [20]. Studies on different water morphologies are also becoming remarkable [21–25]. However, in contrast to water morphologies based on tetramers and hexamers, the water morphologies involving isolated organic hosts are less developed. Exploring new 1-D and 2-D water morphologies based on water pentamers will be interesting but a challenge. In this work, we have obtained two copper(II) complexes, $[Cu(2,2'-bpy)_2(ppac)](H_2O)_7$ (1) and $[Cu_2(2,2'-bpy)_4(ppac)](HCO_2^-)_2(H_2O)_{16}$ (2) based on H_2ppac. An unusual 1-D water tape in complex 1 notated as T4(2)6(2) [26] is stabilized by two zigzag chains of the lipophilic hosts [27] that undergo hydrogen-bonding to adjacent hexamer water rings. We present an unprecedented water morphology in complex 2 defined as T4(1)6(1)6(2), wherein the ratio of water tetramers and hexamers is 1 : 3. Complex cations play important role in the formation of the 3-D structure by supporting adjacent water sheets.

2. Experimental

2.1. *Materials and physical measurements*

All reagents were commercially available and used without purification. Elemental analyses (C, H, and N) were performed on a Vario EL III elemental instrument. IR spectra were recorded from 400 to $4000 \, cm^{-1}$ with KBr pellets on a Shimadzu FTIR-8400 spectrophotometer. Cyclic voltammetry was measured on a CHI860D glassy carbon (GC) electrode as a working electrode, a saturated calomel electrode as a reference electrode, and a platinum wire as an auxiliary electrode. Thermogravimetric analyses (TGA) were performed using a Mettler TGA/SDTA851 thermal analyzer under N_2 with a heating rate of $10°C \, min^{-1}$ from $20°C$ to $1000°C$. Powder X-ray diffraction (PXRD) patterns were collected on a Bruker D8 Avance diffractometer using a graphite-monochromated Cu-Kα radiation ($\lambda = 1.5406 \, Å$).

2.2. *Preparations*

2.2.1. $[Cu(2,2'-bpy)_2(ppac)](H_2O)_7$ **(1).** A solution of p-phenylenediacetic acid (194 mg, 1 mmol) in DMF/water (25 mL, v/v, 1 : 1) was added to a solution of $CuSO_4 \cdot 5H_2O$ (148 mg, 1 mmol) in distilled water (10 mL). After 30 min, 2,2'-bipyridine (312 mg, 2 mmol) was added. The mixture was stirred at room temperature for 15 min and the precipitated product was filtered. Filtrate was kept at room temperature for a month resulting in blue crystals of **1**. Yield: 29%. Anal. Calcd C, 51.91; H, 5.52; N, 8.07%. Found: C, 50.45; H, 5.59; N, 8.68%. FT-IR (cm^{-1}): 3600(vs), 1803(vs), 1472(ms), 1412(ms), 1206(ms), 1087(ms), 979(w), 890(w).

2.2.2. $[Cu_2(2,2'-bpy)_4(ppac)](HCO_2^-)_2(H_2O)_{16}$ **(2).** A solution of p-phenylenediacetic acid (97 mg, 0.5 mmol) in DMF/water (25 mL, v/v, 1 : 1) was added to a solution of $CuSO_4 \cdot 5H_2O$ (148 mg, 1 mmol) in distilled water (10 mL) and after 30 min, 2,2'-bipyridine (312 mg, 2 mmol) was added. The mixture was stirred at room temperature for 15 min, placed in a 25 mL Teflon-lined autoclave and heated at $140°C$ for 120 h. The autoclave was cooled over a period of 11 h at $10°C \, h^{-1}$ and the

product was filtered at ambient temperature to give **2** as blue crystals. Yield: 44%. Anal. Calcd C, 47.23; H, 5.64; N, 8.47%. Found: C, 47.45; H, 5.59; N, 8.44%. FT-IR (cm^{-1}): 3240(vs), 1718(vs), 1561(ms), 1393(ms), 1254(ms), 843(w), 860(w), 713(w).

2.3. *Crystallographic data collection and refinement of the structures*

Crystals suitable for X-ray analyses were grown by slow evaporation of methanol solutions of the complexes. X-ray diffraction data were collected on a Bruker-AXS APEX utilizing Mo-Kα radiation ($\lambda = 0.71073$ Å). The structures were solved by direct methods and refined with full-matrix least-squares. Anisotropic thermal parameters were applied to all nonhydrogen atoms. All hydrogen atoms are located from the difference electron density map and constrained to ideal positions in the refinement procedure. Absorption correction was performed using SADABS [28]. All calculations were performed using SHELX-97 [29]. Crystal data and experimental details for the crystals are summarized in table 1 and hydrogen bonds are given in table 2.

3. Results and discussion

3.1. *Crystal structures of 1 and 2*

Single-crystal X-ray diffraction measurements reveal that complex **1** crystallizes in space group of $P\bar{1}$. Copper atoms are six-coordinate to four nitrogen atoms from 2,2′-bpy and two oxygen atoms from ppac (figure 1a). The ppac coordinates to the copper using only one carboxyl group and with the other carboxyl group deprotonated. The deprotonated

Table 1. Crystal data and structure refinements for **1** and **2**.

Complexes	**1**	**2**
Empirical formula	$C_{30}H_{38}CuN_4O_{11}$	$C_{52}H_{74}Cu_2N_8O_{24}$
Formula weight	694.18	1322.27
Temperature (K)	296(2)	296(2)
Crystal system	Triclinic	Triclinic
Space group	$P\bar{1}$	$P\bar{1}$
Unit cell dimensions (Å, °)		
a	10.371(2)	10.095(3)
b	12.717(2)	12.009(3)
c	14.395(2)	14.651(4)
α	100.700(2)	107.045(3)
β	97.835(2)	156.02(2)
γ	107.019(2)	104.657(4)
V (Å^3)	107.246(2)	1578.9(8)
Z	2	1
D_{Calcd} (g cm^{-3})	1.393	1.391
$F[000]$	726	692
θ (°)	1.55 to 25.01	1.51 to 25.02
μ (mm^{-1})	0.723	0.756
Data/restraints/parameters	5748/0/415	17,763/0/1348
Final R^a indices [$I > 2\sigma(I)$]	$R_1 = 0.0365$, $wR_2 = 0.1080$	$R_1 = 0.0525$, $wR_2 = 0.16672$
R indices (all data)	$R_1 = 0.0412$, $wR_2 = 0.1124$	$R_1 = 0.0689$, $wR_2 = 0.1861$

$^a R_1 = \Sigma(|F_o| - |F_c|)/\Sigma|F_o|$; $wR_2 = [\Sigma w(|F_o^2| - |F_c^2|)^2/\Sigma w(|F_o^2|)^2]^{1/2}$.

Table 2. H-bonded lengths (Å) and angles (°) of **1** and **2**.

D–H···A	d(H···A)	d(D···A)	$\angle$(DHA)	Symmetry code
1				
O5–H5a···O11	1.908	2.756	174.80	$-x+2, -y+2, -z+1$
O5–H5b···O4	1.926	2.774	174.83	
O6–H6a···O1	1.959	2.809	179.89	$-x+1, -y+1, -z+1$
O6–H6b···O3	1.805	2.655	179.68	
O7–H7a···O5	1.982	2.816	166.60	
O7–H7b···O6	1.850	2.683	166.19	
O8–H8a···O10	1.996	2.816	161.87	$x, y, z+1$
O8–H8b···O7	1.941	2.760	161.42	
O9–H9a···O4	1.922	2.768	173.63	$x-1, y, z$
O9–H9b···O8	1.950	2.796	173.96	
O10–H10a···O9	1.897	2.738	169.91	$-x+1, -y+2, -z+1$
O10–H10b···O2	1.877	2.718	170.23	
O11–H11a···O10	1.928	2.749	161.92	
O11–H11b···O7	1.991	2.811	161.75	$x, y, z-1$
2				
O5–H5a···O12	1.988	2.812	163.15	
O5–H5b···O7	2.091	2.918	164.17	$-x+1, -y+1, -z+1$
O7–H7a···O5	2.003	2.847	171.52	$x, y-1, z$
O7–H7b···O10	2.068	2.912	171.71	$-x+1, -y+1, -z+1$
O8–H8a···O3	1.950	2.797	174.28	$-x, -y, -z+1$
O8–H8b···O9	1.941	2.788	174.17	
O9–H9a···O3	1.934	2.781	174.59	$x, y, z-1$
O9–H9b···O10	2.022	2.870	175.05	$-x+1, -y+1, -z+1$
O10–H10a···O2	1.938	2.780	170.37	$-x, -y+1, -z+1$
O10–H10b···O4	1.898	2.740	170.55	$x, y+1, z$
O11–H11c···O4	1.981	2.831	179.17	$-x+1, -y+1, -z+1$
O11–H11d···O5	2.005	2.855	179.40	$-x+1, -y+2, -z+1$
O12–H12a···O11	1.935	2.775	169.67	$x-1, y, z$
O12–H12b···O8	1.900	2.741	169.69	$x, y+1, z$
O6–H6c···O7	2.156	3.004	175.99	
O6–H6d···O11	2.350	3.198	175.59	$-x+1, -y+1, -z+1$

carboxyl group is also evident by nearly identical C–O distances and charge balance. An unusual 1-D water tape notated as T4(2)6(2) is formed by six lattice water molecules and their symmetry equivalent.

Six independent lattice water molecules are connected by hydrogen bonds to form a 1-D hydrogen-bonded water tape along the *a*-axis (figure 2b). These water tapes are located in the gaps of the 2-D networks, which act as a host to stabilize the water tapes. The water tape is puckered with a "z" fashion (figure 2c).

A detailed structure of the water tape, shown in figure 2(a), consists of two water hexamers (O8, O9, O10 and their symmetry equivalents) connected through O10–H10a···O11 and O8–H8a···O7 hydrogen bonds. In this way, one water tetramer is formed by sharing two edges of adjacent water hexamers, resulting in the overall T4(2)6(2) water topology. Carboxyl groups provide potential hydrogen bonding intermolecular interactions, by which two hexamer water clusters are joined by O4. Within the water tape, O···O distances are 2.655–2.816 Å with an average of 2.760 Å, shorter than that observed in the ice Π-phase of 2.77–2.84 Å [30]. The O···O···O angles vary from 161.42° to 179.89°.

Single-crystal X-ray diffraction measurement reveals that complex **2** crystallizes in space group of $P\bar{1}$. Copper has a distorted octahedral geometry by coordinating with
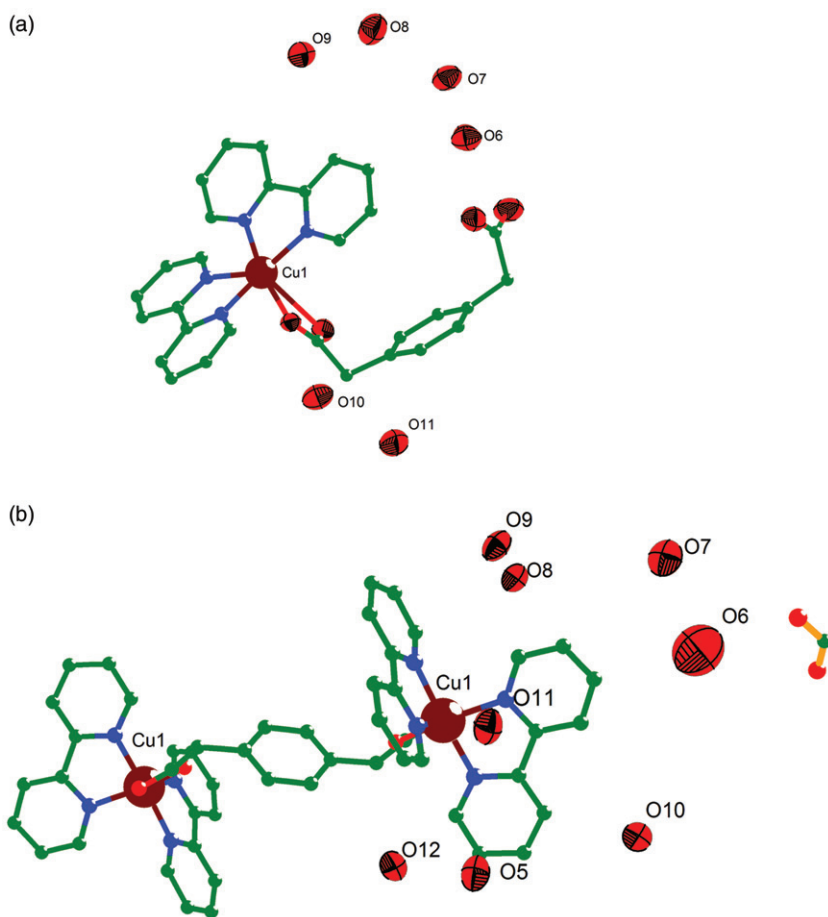
Figure 1. The coordination environments of Cu with 50% thermal ellipsoids for (a) **1** and (b) **2**. All hydrogen atoms are omitted for clarity.

four nitrogen atoms from 2,2′-bpy and two oxygen atoms from carboxyl of ppac (figure 1b). The ppac coordinates with copper by using both carboxyl groups, different than **1**. The ratios of initial reactants and reaction temperature play important role in the formation of different structures of **1** and **2**, though the reaction source and conditions are the same. Taking into account of the imbalance of the charge, deprotonated HCO_2^- is suggested for the isolated ions, formed by decomposition of DMF at high temperature; eight lattice water molecules are contained in **2**.

The water cluster is shown in figure 3(b), $H_2O(5)$, $H_2O(11)$, and $H_2O(12)$ compose a water hexamer, while $H_2O(5)$ and $H_2O(7)$ compose a water tetramer by H-bonds O5–H5a···O12, O11–H11d···O5, O12–H12a···O11, O5–H5b···O7, and O7–H7a···O5. As shown in figure 3(b), adjacent tetramers and hexamers share $H_2O(5)$ to create a T4(1)6(1) tape in which O5 displays four H-bonds. The other type of water hexamer consists of $H_2O(5)$, $H_2O(7)$, $H_2O(8)$, $H_2O(9)$, $H_2O(10)$, and $H_2O(12)$ through hydrogen bonds of O8–H8b···O9, O7–H7b···O10, O9–H9b···O10, O12–H12a···O11, and O12–H12b···O8. Water hexamers are combined to give a T6(2) water tape via
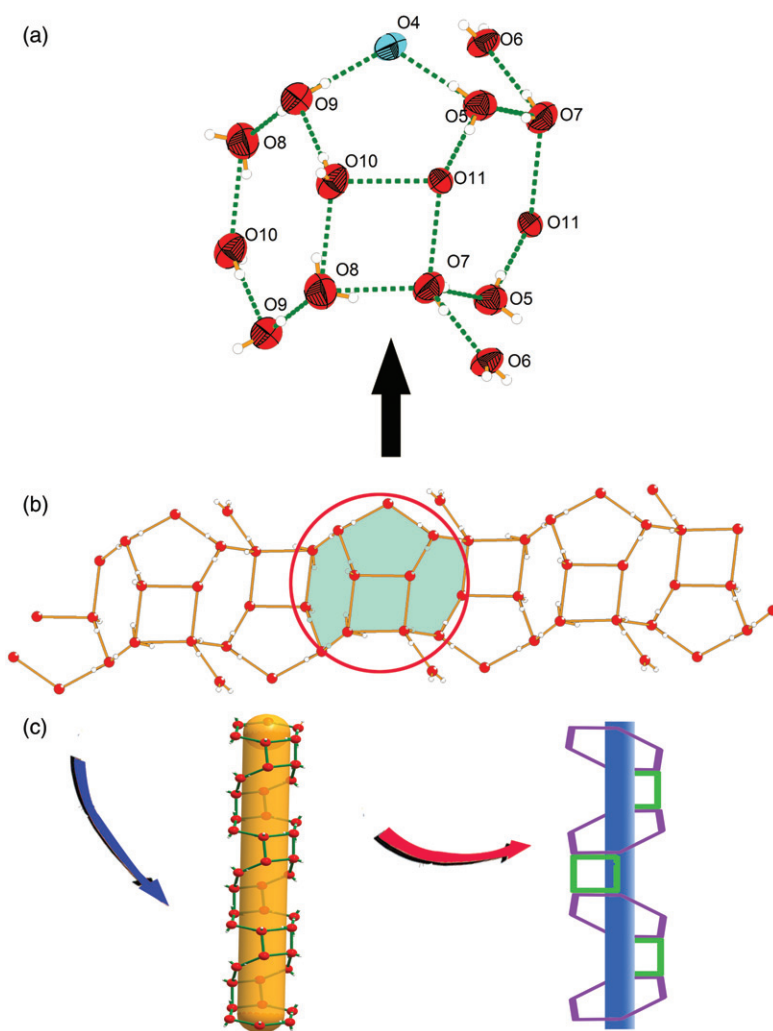
Figure 2. (a) Water hexamer embedded in the gaps of the channel. (b) Perspective view of supramolecular $(H_2O)_n$ morphology in **1**. (c) Packing diagram of the hexamer water clusters.

sharing two edges of adjacent hexamer. Combined with the T4(1)6(1) water structure, the overall water structure is defined as T4(1)6(1)6(2) tape [31].

Deprotonated formic acid and lattice waters are held together forming hydrogen-bonded layers as shown in figure 3(b) and (c). The 2-D layers are separated by $[Cu_2(2,2'-bpy)_4]^{2+}$ resulting in a 3-D framework. In this system [32], uncoordinated formate is a host, at the same time acting as a guest of the stacking structure of complex **2**. In other organic-water clusters, organic compound always acts a host and such dual host–guest features including water clusters are very rare [33]. For the first time, a layer structure built on water cluster and organic guest (formate) are observed. In addition, π–π stacking interactions provide further stability between adjacent complex ions and form zigzag chains in the channel formed by the water sheet (figure 4).
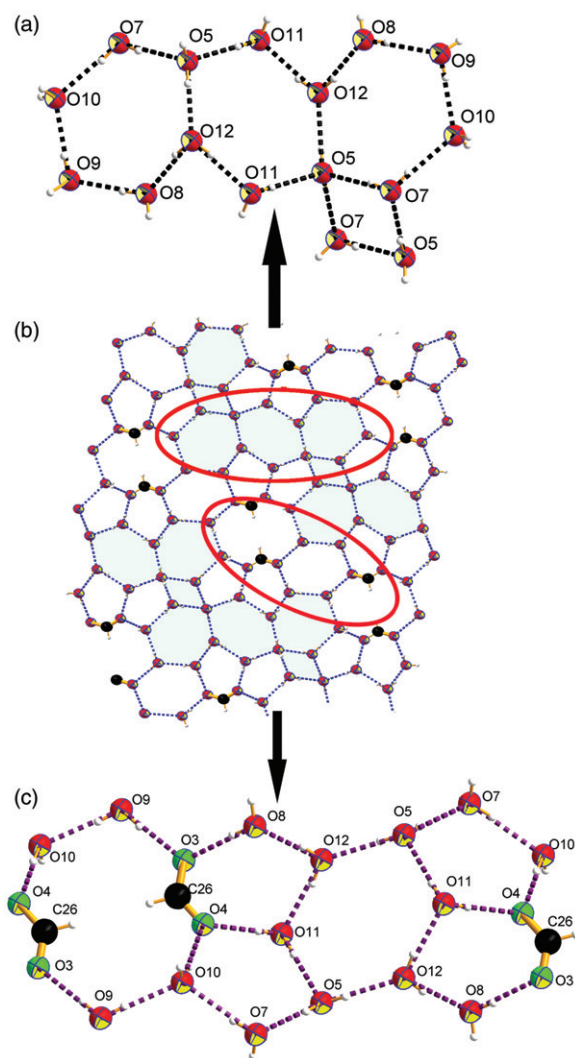
Figure 3. (a) Packing diagram of the hexamer and tetramer water clusters. (b) Perspective view of supramolecular $(H_2O)_n$ morphology in **2**. (c) Hydrogen bonds between the HCO_2^- and lattice waters.

The hydrophobic host is embedded in the cage formed by the hydrophilic guest molecules. The supramolecular assembly of $2HCO_2^-$ with $[Cu_2(2,2'-bpy)_4]^{2+}$ forms a negatively charged cage as shown in figure 5(a) and (b). In this cage, the lattice water molecules accept hydrogen atoms of 2,2'-bpy, resulting in multiple interactions. Meanwhile, $[Cu_2(2,2'-bpy)_4]^{2+}$ are pillars which supported the negative charged layers at 10.349 Å.

3.2. *Electrochemistry*

The electrochemical behavior of complex **2** in DMSO was examined by using cyclic voltammetry from −0.6 to 0.8 V. The resulting cyclic voltammogram (CV) is shown in
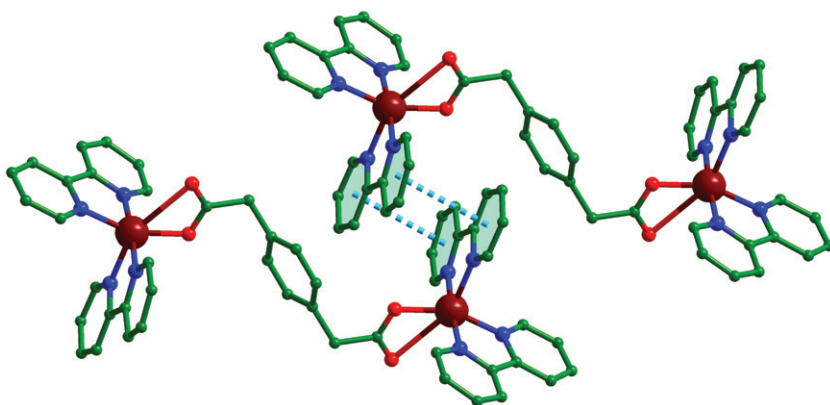
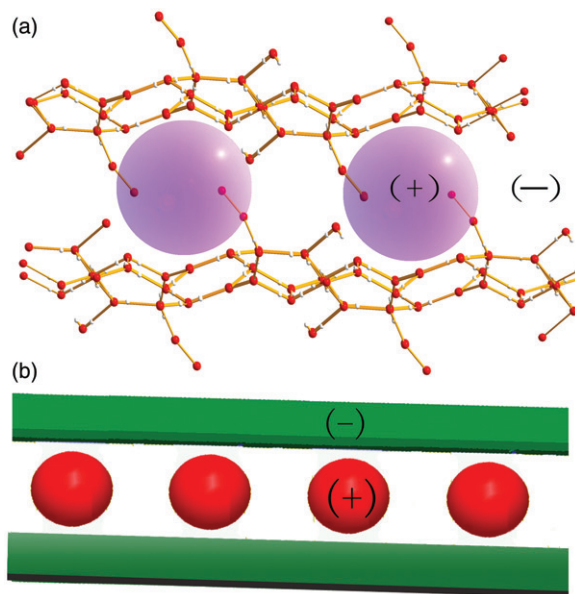Figure 4. 1-D zigzag chains formed by the π–π stacking interactions between 2,2′-bpy molecules.

Figure 5. Model of the 3-D structure showing the frameworks formed by the guest molecules (pillar-layer structure) with negative charge (a) and host (red ball) with positive charge (b). (For interpretation of the references to color in this figure legend, the reader is referred to the web version of this article.)

"Supplementary material." Complex **2** displays a couple of quasi-reversible oxidation and reduction waves with reduction potential at 0.05 V and the oxidation potential at −0.36 V. The reduction and oxidation were assigned to the Cu^{II}/Cu^{I} couple according to the literature [34–37].

3.3. *Thermal decomposition*

TGA indicates that complex **1** loses 19% of total weight at 50°C–120°C, corresponding to the removal of seven lattice water molecules per formula unit (Calcd 18%).

The product loses 62% of total weight at 180°C–240°C, corresponding to decomposition of the ligands. Complex **2** exhibits an initial weight loss of 19% at 50°C–90°C, corresponding to the removal of 16 lattice water molecules per formula unit (Calcd 21%), followed immediately by 5.5% weight loss between 90°C and 150°C, from removal of the formate. The third stage with 50% mass loss starts at 150°C and finishes at 220°C, for a loss of 2,2′-bpy from the complex. The residual weight after decomposition is consistent with the formation of CuO. The structures are also characterized by PXRD pattern, which match well with the simulated pattern (Supplementary material).

4. Conclusion

We prepared and characterized $[Cu(2,2'\text{-bpy})_2(ppac)](H_2O)_7$ (**1**) and $[Cu_2(2,2'\text{-bpy})_4]$ $(HCO_2^-)_2(H_2O)_{16}$ (**2**). Hydrogen bond interactions and related forces contribute to the formation of the packing structures. Unusual water morphologies are present in the complexes that are discussed here.

Supplementary material

Crystallographic data (excluding structure factors) for the structures in this article have been deposited with the Cambridge Crystallographic Data Centre as supplementary publications CCDC 857181 and 857182. Copies of the data can be obtained free of charge on application to CCDC, 12 Union Road, Cambridge CB2 1EZ, UK [Fax: 441223-336-033; E-mail: deposit@ccdc.cam.ac.uk.].

References

[1] R. Ludwig. *Angew. Chem., Int. Ed.*, **40**, 1808 (2001).
[2] S.S. Xantheas. *J. Chem. Phys.*, **100**, 7523 (1994).
[3] J. Kim, K.S. Kim. *J. Chem. Phys.*, **109**, 5886 (1998).
[4] L.R. MacGillivray, J.L. Atwood. *J. Am. Chem. Soc.*, **119**, 2592 (1997).
[5] S. Noro, R. Kitaura, M. Kondo, S. Kitagawa, T. Ishii, H. Matsuzaka, M. Yamashita. *J. Am. Chem. Soc.*, **124**, 2568 (2002).
[6] S. Neogi, G. Savitha, P.K. Bharadwaj. *Inorg. Chem.*, **43**, 3771 (2004).
[7] C.J. Gruenloh, J.R. Carney, C.A. Arrington, T.S. Zwier, S.Y. Fredericks, K.D. Jordan. *Science*, **276**, 1678 (1997).
[8] L. Infantes, J. Chisholm, S. Motherwell. *CrystEngComm*, **5**, 480 (2003).
[9] X. Li, X. Qiu. *J. Coord. Chem.*, **63**, 4077 (2010).
[10] K. Zhao, Y. Jiang, X. Qiu, J. Tian, X. Li. *J. Coord. Chem.*, **64**, 1375 (2011).
[11] H. Liu, H. Wang, Y. Shi. *J. Coord. Chem.*, **64**, 2859 (2011).
[12] P.S. Lakshminarayanan, E. Suresh, P. Ghosh. *J. Am. Chem. Soc.*, **127**, 13132 (2005).
[13] F. Hu, X. Yin, Y. Mi, J. Zhang, Y. Zhuang, X. Dai. *Inorg. Chem. Commun.*, **12**, 628 (2009).
[14] F. Hu, X. Yin, Y. Mi, S. Zhang, W. Luo, Y. Zhuang. *Inorg. Chem. Commun.*, **12**, 1189 (2009).
[15] F. Hu, X. Yin. *Inorg. Chem. Commun.*, **15**, 256 (2012).
[16] R.E. Dehl, C.A. Hoeve. *J. Chem. Phys.*, **50**, 3245 (1969).
[17] S. Dalai, A. Rana, D. Chowdhuri, M. Bera, E. Zangrando. *Inorg. Chim. Acta*, **363**, 1052 (2010).
[18] S.D. Colson, T.H. Dunning. *Science*, **265**, 43 (1994).

[19] G.M. Sun, J. Zou, Z.W. Liao, G.L. Yan, H.X. Huang, S.J. Liu, F. Luo. *Inorg. Chem. Commun.*, **14**, 1283 (2011).
[20] S. Pal, N.B. Sankaran, A. Samanta. *Angew. Chem. Int. Ed.*, **42**, 1741 (2003).
[21] S. Supriya, S. Manikumari, P. Raghavaiah, S.K. Das. *New J. Chem.*, **27**, 218 (2003).
[22] G.E. Kostakis, G. Abbas, C.E. Anson, A.K. Powell. *CrystEngComm*, **10**, 1117 (2008).
[23] M.V. López, G. Zaragoza, M. Otero, R. Pedrido, G. Rama, M.R. Bermejo. *Cryst. Growth Des.*, **8**, 2083 (2008).
[24] R.Q. Zhong, R.Q. Zou, M. Du, N. Takeichi, Q. Xu. *CrystEngComm*, **10**, 1175 (2008).
[25] LY. Wang, Y. Yang, K. Liu, B.L. Li, Y. Zhang. *Cryst. Growth Des.*, **8**, 3902 (2008).
[26] L. Infantes, J. Chisholm, S. Motherwell. *CrystEngComm*, **5**, 480 (2003).
[27] X. Mei, C. Wolf. *CrystEngComm*, **8**, 337 (2006).
[28] G.M. Sheldrick. *SADABS (Version 2007/4)*, Bruker AXS Inc., Madison, WI (2007).
[29] G.M. Sheldrick. *Acta Cryst.*, **A64**, 112 (2008).
[30] J.K. Gregory, D.C. Clary, K. Liu, M.G. Brown, R.J. Saykally. *Science*, **275**, 814 (1997).
[31] X. Tian, Y. Song, G. Sun, H. Huang, W. Xu, X. Feng, F. Luo. *Inorg. Chem. Commun.*, **15**, 252 (2012).
[32] S. Banerjee, R. Murugavel. *Cryst. Growth Des.*, **4**, 545 (2004).
[33] J. Sun, H. Xu. *Inorg. Chem. Commun.*, **14**, 254 (2011).
[34] M. Thirumavalavan, P. Akilan, M. Kandaswamy, K. Chinnakali, G.S. Kumar, H.K. Fun. *Inorg. Chem.*, **42**, 3308 (2003).
[35] R.J. Crutchley, R. Hynes, E.J. Gabe. *Inorg. Chem.*, **29**, 4921 (1990).
[36] J. Casanova, G. Alzuet, J. Latorre, J. Borrá. *Inorg. Chem.*, **36**, 2052 (1997).
[37] A. Widmann, H. Kahlert, I. Petrovic-Prelevic, H. Wulff, J.V. Yakhmi, N. Bagkar, F. Scholz. *Inorg. Chem.*, **41**, 5706 (2002).